NANOSYSTEMS:
PHYSICS, CHEMISTRY, MATHEMATICS

Original article

Dorosheva I.B., et al. *Nanosystems: Phys. Chem. Math.*, 2023, **14** (4), 447–453.
http://nanojournal.ifmo.ru
DOI 10.17586/2220-8054-2023-14-4-447-453

Induced surface photovoltage in TiO_2 sol-gel nanoparticles

Irina B. Dorosheva[1,2,a], Alexander S. Vokhmintsev[1,b], Ilya A. Weinstein[1,2,c], Andrey A. Rempel[1,2,d]

[1]Ural Federal University, Yekaterinburg, Russia

[2]Institute of Metallurgy of the Ural Branch of the Russian Academy of Sciences, Yekaterinburg, Russia

[a]i.b.dorosheva@urfu.ru, [b]a.s.vokhmintsev@urfu.ru, [c]i.a.weinstein@urfu.ru, [d]rempel.imet@mail.ru

Corresponding author: I. B. Dorosheva, i.b.dorosheva@urfu.ru

ABSTRACT TiO_2 nanoparticles synthesized by the sol-gel method and modified by annealing in air and hydrogen atmospheres were studied by surface photovoltage spectroscopy (SPS). SPS measurements showed that the modified in air TiO_2 nanoparticles have a more intense signal than those treated in hydrogen. A linear correlation was found between the SPS and the diffuse reflectance spectra of the samples.

KEYWORDS Titanium dioxide, sol-gel method, nanoparticles, surface photovoltage (SPV).

ACKNOWLEDGEMENTS A.S.V. and I.A.W. thank the Ministry of Science and Higher Education of the Russian Federation (research project FEUZ-2023-0014) for support. Part of synthesis of titanium dioxide carried out within the framework of RF State assignment for IMET UB RAS.

FOR CITATION Dorosheva I.B., Vokhmintsev A.S., Weinstein I.A., Rempel A.A. Induced surface photovoltage in TiO_2 sol-gel nanoparticles. *Nanosystems: Phys. Chem. Math.*, 2023, **14** (4), 447–453.

1. Introduction

Titanium dioxide has attracted the attention of scientists around the world for many years, because it is a chemically stable, non-toxic, and inexpensive material that has functional properties for use as photocatalysts in the decomposition of toxicants [1–4], photosorbents of rare earth elements [5–7], renewable energy sources [8–10], resistive memory elements [11–13], new organic compounds synthesis for medicine [14–16], etc. There are also various ways for the nanosized titanium dioxide synthesis: solvothermal [17–19], hydrothermal [20–22], anodic oxidation [2, 23, 24], chemical vapor deposition [25–27], electrodeposition [28–31], sonochemical [32–35], and microwave methods [36–39]. However, TiO_2 has a wide bandgap of 3.0–3.3 eV [40, 41], which makes it difficult to apply it as a photosorbent and photocatalyst under visible light irradiation. In this regard, the material is modified in various ways: by creating a heterostructure, doping with metal ions, annealing in atmospheres of air, hydrogen, argon, nitrogen, etc. [42–49] to create atomic defects and surface states capable to capture photons with lower energy. One of the instruments for study such states is the surface photovoltage spectroscopy (SPS), which allows a non-contact, non-destructive and highly sensitive way to determine the electronic features in surface of solids and can be used to analyze charges separation and transfer in the mechanisms of photocatalysis, dye sensitization, etc. [50–55]. The method is based on the generation of voltage by a capacitor structure with a sample under study between electrodes upon excitation by light [52] and is a suitable tool for study photophysical processes in nanoscale semiconductors for several reasons. First, the SPS is generated as a result of band-to-band transitions, which makes it possible to estimate the semiconductor bandgap [52]. Second, the method is sensitive to band-to-band transitions due to the surface states of a material, which, as a rule, arise due to impurities or point defects in its structure. Therefore, the aim of this work is to study the titanium dioxide nanoparticles, synthesized by the sol-gel method, via surface photovoltage spectroscopy.

2. Samples and experiment

TiO_2 nanoparticles were obtained by the sol-gel method at the initial solution pH of 2, 6, and 8, followed by annealing in air in an SNOL 6.7/1300 muffle furnace at a temperature of 350°C for 4 hours [15,43,56,57]. Also, the sample obtained at $pH = 6$ was annealed in an MPT-2MR tube furnace in a hydrogen atmosphere at temperatures of 200, 400 and 600°C for 60 minutes [43]. The synthesized TiO_2 nanoparticles were previously studied using X-ray phase analysis, diffuse reflectance spectroscopy, and the Brunauer-Emmett-Teller (BET) method [15, 43, 56, 57] (see Table 1).

The surface photovoltage (SPV) spectra were investigated using the measuring installation based on an LS 55 luminescent spectrometer (Perkin-Elmer, USA) with the developed electroluminescent cell [58] and a PXI-4071 digital multimeter (National Instruments, USA). The SPS measurements were controlled by the original virtual device developed in the LabVIEW programming environment. The studied TiO_2 samples were placed between the transparent ITO glass electrode and the $Sn_{0.61}Cu_{0.39}$ electrode (Fig. 1).

The distance between the electrodes was $d \approx 20$ μm. To generate photovoltage, the sample was excited by monochromatic light from a pulsed Xe lamp in the range of 290–450 nm at a monochromator exit slit of 10 nm and a scanning rate

TABLE 1. Characteristics of titanium dioxide powders [15,43,56,57]

Sample	pH of sol			Annealing temperature in H_2			Degussa P25	Hombifine
	2	6	8	200°C	400°C	600°C		
Phase composition	Anatase			Amorphous	Anatase		Anatase, rutile	Anatase
Coherent scattering region ±10 %, nm	8	9	20	–	46	36	25	15
$S_{BET} \pm 2$ %, m^2/g	140	140	90	310	120	40	55	70
$E_g \pm 0.1$, eV	3.0	3.2	3.2	3.3	3.2	3.2	3.0	3.3

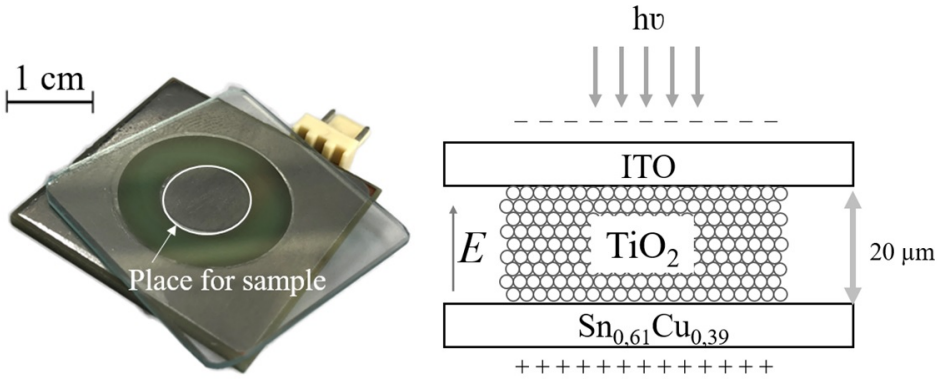

FIG. 1. Image and scheme of a cell for measuring SPV

of 1 nm/s. The SPS signal was recorded by a digital multimeter with a period of 250 ms. Since electrodes with different materials were used, differing in the work function $A_{out} \approx 4.8$ eV (ITO) and 4.4 eV (Cu, Sn), under the conditions of the induced internal electric field, the background SPS signal was recorded in the dark. Taking into account the emerging contact potential difference of 0.4 eV and the sample thickness d, the induced electric field was $E = 2 \cdot 10^6$ V/cm. In this regard, the indicated background SPS signal was subtracted when processing the initial experimental data. The resulting SPS curves were normalized to the ITO transmission spectrum (Fig. 2).

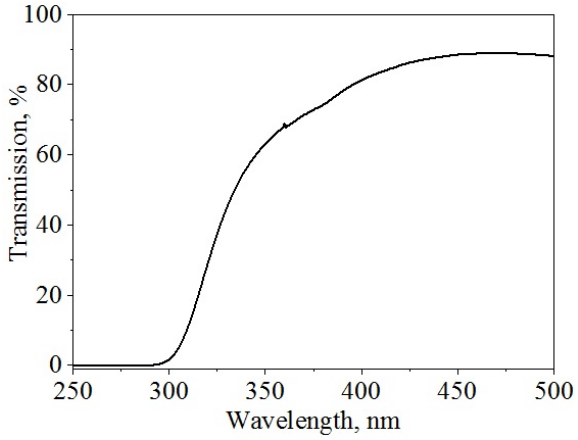

FIG. 2. ITO transmission spectrum

3. Results and discussion

The SPS of the studied samples are shown in Figs. 3-4. Hombifine powder was measured for the first time (Fig. 3), there are no data in the literature on measuring its properties by this method. The absolute changes in induced photovoltage ΔU_{max} (Fig. 4) depending on the excitation wavelength for samples annealed in air ($\Delta U_{max} \approx 150$ mV) are almost two times higher than for samples annealed in hydrogen ($\Delta U_{max} \approx 60 \div 80$ mV).

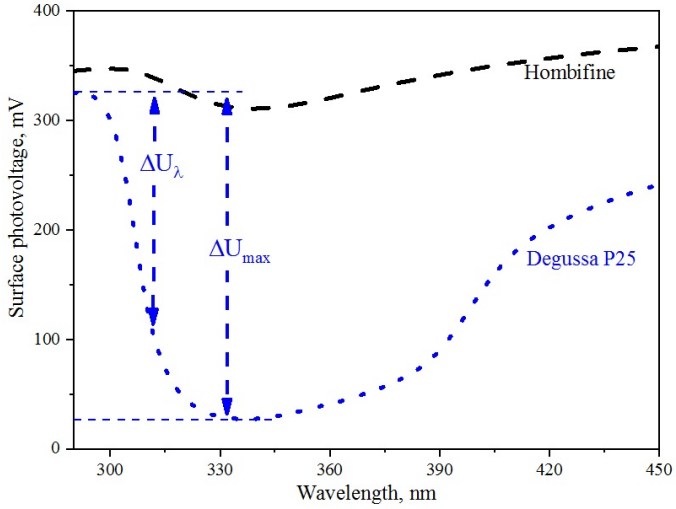

FIG. 3. SPV spectra of Degussa P25 and Hombifine powders

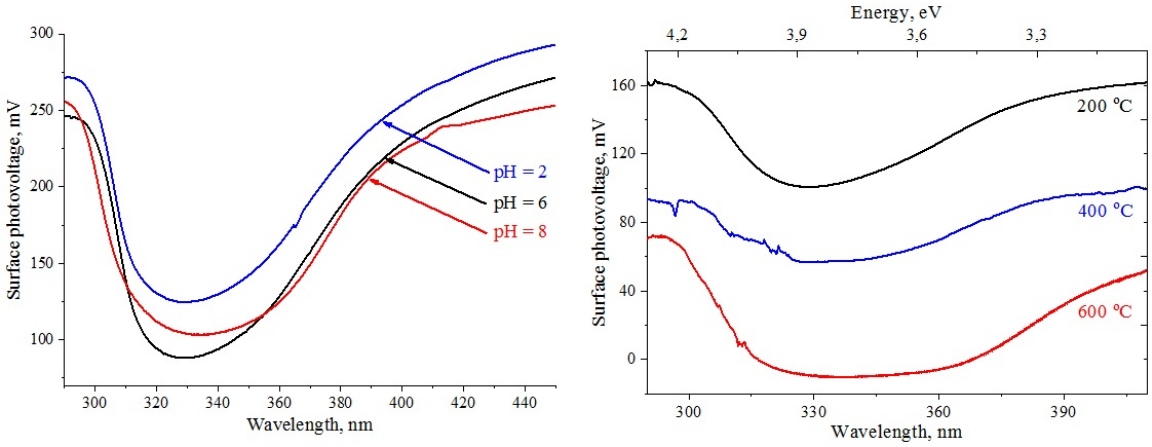

FIG. 4. SPV spectra of TiO_2 samples obtained by the sol-gel method

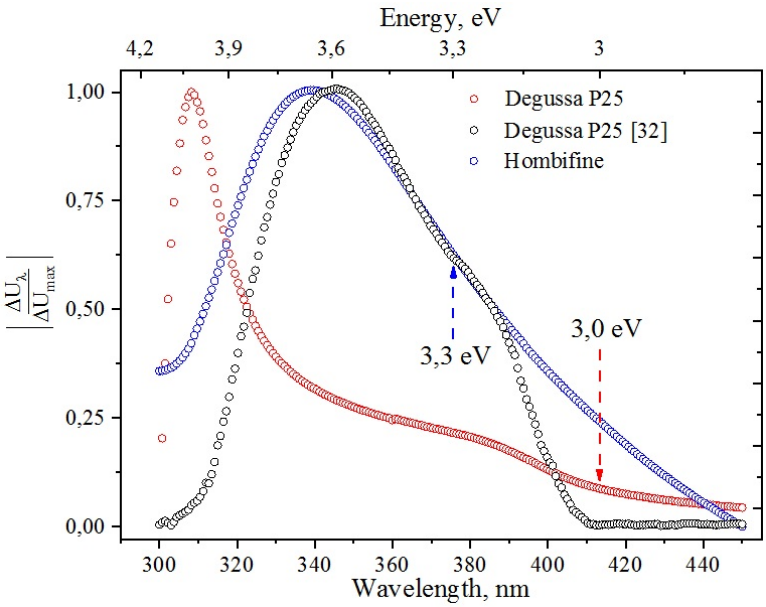

FIG. 5. Normalized surface photovoltage spectra for Degussa P25 and Hombifine powders

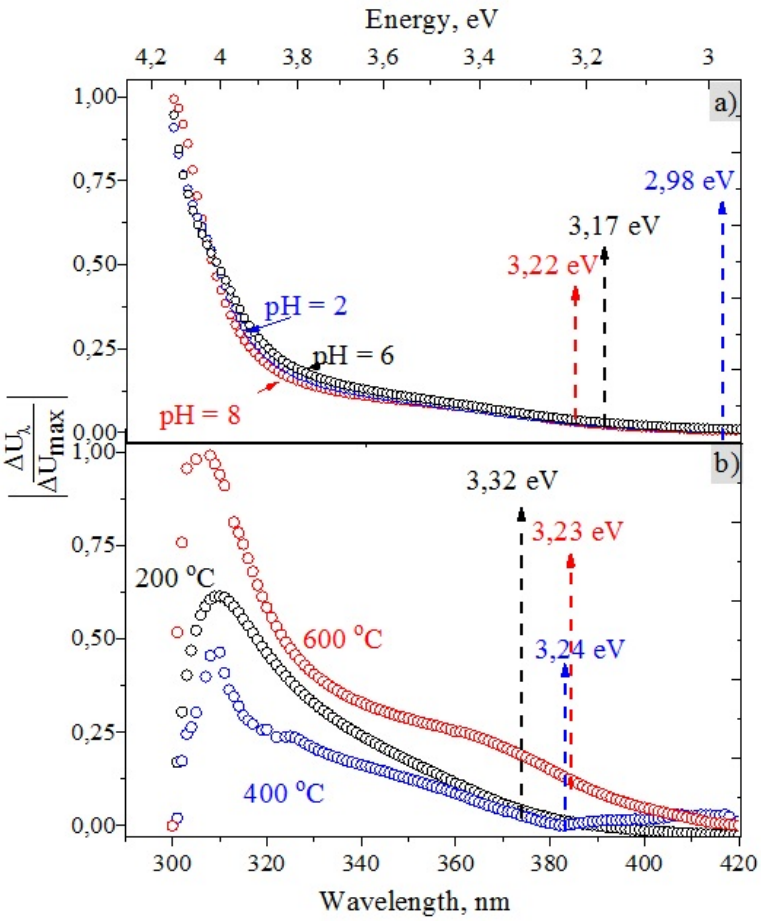

FIG. 6. Normalized surface photovoltage spectra of TiO_2 samples obtained by the sol-gel method

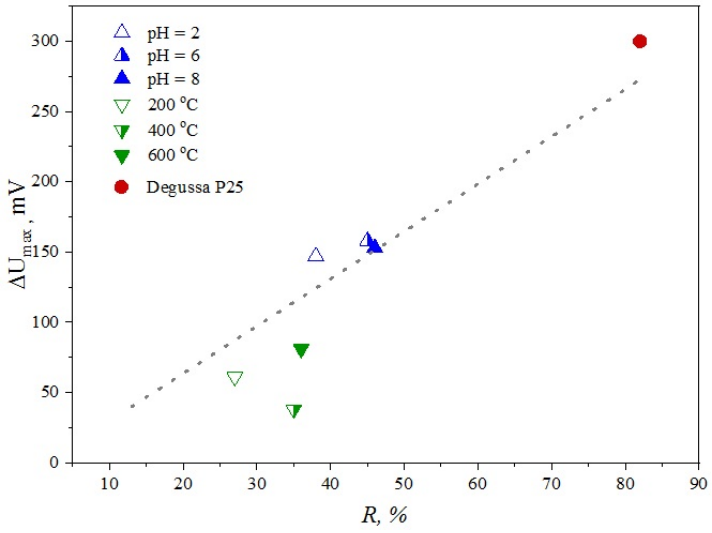

FIG. 7. The dependence of the SPS signal ΔU_{max} on the reflectance R at a 430 nm wavelength

After annealing TiO_2 nanoparticles in air, the SPS spectra have a similar shape, regardless of the sol pH during their synthesis. Comparing the studied samples, it can be noted that the highest value of ΔU_{max} appears after annealing in air. This is due to the complete crystallization of the samples to anatase symmetry and a decrease of the vacancies concentration upon annealing in air. Upon annealing in a reducing hydrogen atmosphere, both with partial and complete crystallization, the oxygen vacancies concentration remains high in the sample structure. Charge carriers are localized on these defects, reducing the ΔU_{max} value. The highest ΔU_{max} among those annealed in hydrogen is demonstrated by the sample treated at 600°C. It is probably due to more efficient separation of electron-hole pairs due to complete crystallization to the anatase phase. A low ΔU_λ value indicates inefficient separation of photoinduced electron-hole pairs or their capture by defect states. Upon annealing at 200°C, the amorphous structure is saved and $\Delta U_{max} \approx 60$ mV. When the temperature rises to 400°C – $\Delta U_{max} \approx 40$ mV incomplete crystallization of TiO_2 to anatase occurs at this temperature. As a result of the presence of boundaries in such a two-phase structure, the migration of charge carriers to the surface is hindered; therefore, ΔU_{max} is smaller than in amorphous TiO_2. Annealing at 600°C leads to increase $\Delta U_{max} \approx 80$ mV. This value is higher than that of amorphous TiO_2 obtained at 200°C. Complete crystallization of the sample to anatase at 600°C leads to the vacancy defects concentration decrease, a more efficient separation of the electron-hole pair and, consequently, a change in the surface charge.

It was found (Fig. 5) that Degussa P25 powder has a maximum photoinduced response in the region of 310 nm, which corresponds to band-to-band optical transitions [59, 60]. The Degussa P25 SPS spectra measured in this work and in [61] differ in the peak position (see Fig. 5). In the cited work, the maximum is shifted to the long wavelength region of 340 nm. This is due to the difference in the materials used for the photovoltaic cell electrodes: two ITO glasses in [61]; in our work, one of the cell electrodes is ITO glass, and the second one is $Sn_{0.61}Cu_{0.39}$ alloy. The work function of these materials differs by ≈ 0.4 eV. Therefore, in our case, additional energy is required to separate the electron-hole pair and release the charge to the surface for signal registration. The corresponding shift in the SPS spectra (Fig. 5) clearly demonstrates this fact. It was also found that Hombifine powder has a maximum photoinduced response in the excitation region of 340 nm. It means that for the separation of electron-hole pairs and the release of charge carriers to the surface, less energy is required than for Degussa P25. This is probably due to the single-phase anatase structure of the sample, i.e. there is no charge carriers scattering at the interphase boundaries of rutile and anatase, which can be characteristic for Degussa P25. The arrows in Figs. 5-6 indicate the bandgap energies of the samples. In addition, a linear relationship was found between the SPS signal and the diffuse reflectance at a wavelength of 430 nm (see Fig. 7) with a Pearson's correlation coefficient of $r = 0.88$.

Thus, the structural and phase features of stoichiometric TiO_2 nanoparticles, which are characterized by a single-phase composition, as well as a low concentration of vacancy and surface defects, significantly affect the efficiency of charge carrier separation processes during band-to-band optical excitation and the formation of SPV. Note that a controlled change in the nanostructures surface charge is great importance for optimizing their photovoltaic properties.

4. Conclusions

In this work, we study the photovoltaic properties of titanium dioxide nanoparticles synthesized by the sol-gel method and modified by annealing in air and in hydrogen atmospheres. According to the increment SPV spectra ΔU_λ, it was found that the nanoparticles modified in air have a more intense signal compared to those treated in hydrogen. Due to the high concentration of oxygen vacancies formed as a result of annealing in a reducing atmosphere, defect states appeared, on which excited electrons are localized, which 2 times weakens the SPV signal. A linear correlation of the SPS data with the diffuse reflection spectra (Pearson's correlation coefficient $r = 0.88$) was found, which also confirms the efficiency of electron-hole pairs separation and changes in the surface charge, provided that the structure is stoichiometric and with the least number of defects.

References

[1] Valeeva A.A., Dorosheva I.B., Kozlova E.A., Kamalov R.V., Vokhmintsev A.S., Selishchev D.S., Saraev A.A., Gerasimov E.Y., Weinstein I.A., Rempel A.A. Influence of Calcination on Photocatalytic Properties of Nonstoichiometric Titanium Dioxide Nanotubes. *Journal of Alloys and Compounds*, 2019, **796**, P. 293–299.

[2] Valeeva A.A., Kozlova E.A., Vokhmintsev A.S., Kamalov R.V., Dorosheva I.B., Saraev A.A., Weinstein I.A., Rempel A.A. Nonstoichiometric Titanium Dioxide Nanotubes with Enhanced Catalytical Activity under Visible Light. *Scientific Reports*, 2018, **8**(1), P. 1–10.

[3] Sreekantan S., Hazan R., Lockman Z. Photoactivity of Anatase-Rutile TiO_2 Nanotubes Formed by Anodization Method. *Thin Solid Films*, 2009, **518**(1), P. 16–21.

[4] Camacho-Muñoz D., Lawton L.A., Edwards C. Degradation of Okadaic Acid in Seawater by UV/TiO_2 Photocatalysis – Proof of Concept. *Science of The Total Environment*, 2020, **733**, P. 139346.

[5] Melchakova O.V., Pechishcheva N.V., Korobitsyna A.D. Mechanically Activated Rutile and Its Sorption Properties with Regard to Gallium and Germanium. *Tsvetnye Metally*, 2019, **1**, P. 32–39.

[6] Method for obtaining a sorbent based on nanosized titanium dioxide. Method for obtaining a sorbent based on nanosized titanium dioxide: Patent 2790032 Russia B01J20/06 B01J20/30 C02F1/28 C02F1/62 B82B3/00. Dorosheva I.B., Pechishcheva N.V., Rempel A.A., patent holder, N 2790032.

[7] Miller S.M., Spaulding M.L., Zimmerman J.B. Optimization of Capacity and Kinetics for a Novel Bio-Based Arsenic Sorbent, TiO_2-Impregnated Chitosan Bead. *Water Research*, 2011, **45**(17), P. 5745–5754.

[8] Valeeva A.A., Dorosheva I.B., Kozlova E.A., Sushnikova A.A., Kurenkova A.Y., Saraev A., Schroettner H., Rempel A. Solar Photocatalysts Based on Titanium Dioxide Nanotubes for Hydrogen Evolution from Aqueous Solutions of Ethanol. *International Journal of Hydrogen Energy*, 2021, **46**(32), P. 16917–16924.

[9] Zheng L., Teng F., Ye X., Zheng H., Fang X. Photo/Electrochemical Applications of Metal Sulfide/TiO_2 Heterostructures. *Advanced Energy Materials*, 2020, **10**(1), P. 1902355.

[10] Kapilashrami M., Zhang Y., Liu Y.S., Hagfeldt A., Guo J. Probing the Optical Property and Electronic Structure of TiO_2 nanomaterials for Renewable Energy Applications. *Chemical Reviews*, 2014, **114**(19), P. 9662–9707.

[11] Vokhmintsev A.S., Weinstein I.A., Kamalov R.V., Dorosheva I.B. Memristive Effect in a Nanotubular Layer of Anodized Titanium Dioxide. *Bulletin of the Russian Academy of Sciences: Physics*, 2014, **78**(9), P. 932–935.

[12] Lettieri S., Pavone M., Fioravanti A., Amato L.S., Maddalena P. Charge Carrier Processes and Optical Properties in TiO_2 and TiO_2-Based Heterojunction Photocatalysts: A Review. *Materials*, 2021, **14**(7), P. 1–57.

[13] Dash C.S., Sahoo S., Prabaharan S.R.S. Resistive Switching and Impedance Characteristics of M/TiO_{2-x}/TiO_2/M Nano-Ionic Memristor. *Solid State Ionics*, 2018, **324**, P. 218–225.

[14] Dorosheva I.B., Valeeva A.A., Rempel A.A., Trestsova M.A., Utepova I.A., Chupakhin O.N. Synthesis and Physicochemical Properties of Nanostructured TiO_2 with Enhanced Photocatalytic Activity. *Inorganic Materials*, 2021, **57**(5), P. 503–510.

[15] Dorosheva I.B., Rempel A.A., Trestsova M.A., Utepova I.A., Chupakhin O.N. Synthesis of a TiO_2 Photocatalyst for Dehydrogenative Cross-Coupling of (Hetero)Arenes. *Inorganic Materials*, 2019, **55**(2), P. 155–161.

[16] Elsayed D.A., Assy M.G., Mousa S.M., El-Bassyouni G.T., Mouneir S.M., Shehab W.S. TiO_2 Nanoparticle as Catalyst for an Efficient Green One-Pot Synthesis of 1H-3-Indolyl Derivatives as Significant Antiviral Activity. *Bioorganic Chemistry*, 2022, **124**, P. 105805.

[17] Ye Y., Feng Y., Bruning H., Yntema D., Rijnaarts H.H.M. Photocatalytic Degradation of Metoprolol by TiO_2 Nanotube Arrays and UV-LED: Effects of Catalyst Properties, Operational Parameters, Commonly Present Water Constituents, and Photo-Induced Reactive Species. Applied Catalysis B: Environmental, 2018, **220**, P. 171–181.

[18] Niu B., Wang X., Wu K., He X., Zhang R. Mesoporous Titanium Dioxide: Synthesis and Applications in Photocatalysis, Energy and Biology. *Materials*, 2018, **11**(10), P. 1–23.

[19] He F., Li J., Li T., Li G. Solvothermal Synthesis of Mesoporous TiO_2: The Effect of Morphology, Size and Calcination Progress on Photocatalytic Activity in the Degradation of Gaseous Benzene. *Chemical Engineering Journal*, 2014, **237**, P. 312–321.

[20] Macak J.M., Hildebrand H., Marten-Jahns U., Schmuki P. Mechanistic Aspects and Growth of Large Diameter Self-Organized TiO_2 Nanotubes. *Journal of Electroanalytical Chemistry*, 2008, **621**(2), P. 254–266.

[21] Tay Q., Liu X., Tang Y., Jiang Z., Sum T.C., Chen Z. Enhanced Photocatalytic Hydrogen Production with Synergistic Two-Phase Anatase/Brookite TiO_2 Nanostructures. *Journal of Physical Chemistry C*, 2013, **117**(29), P. 14973–14982.

[22] Liu N., Chen X., Zhang J., Schwank J.W. A Review on TiO_2-Based Nanotubes Synthesized via Hydrothermal Method: Formation Mechanism, Structure Modification, and Photocatalytic Applications. *Catalysis Today*, 2014, **225**, P. 34–51.

[23] Rempel A.A., Valeeva A.A., Vokhmintsev A.S., Weinstein I.A. Titanium Dioxide Nanotubes: Synthesis, Structure, Properties and Applications. *Russian Chemical Reviews*, 2021, **90**(11), P. 1397–1414.

[24] Zhou X., Nguyen N.T., Özkan S., Schmuki P. Anodic TiO_2 Nanotube Layers: Why Does Self-Organized Growth Occur—A Mini Review. *Electrochemistry Communications*, 2014, **46**, P. 157–162.

[25] Sotelo-Vazquez C., Quesada-Cabrera R., Darr J.A., Parkin I.P. Single-Step Synthesis of Doped TiO_2 Stratified Thin-Films by Atmospheric-Pressure Chemical Vapour Deposition. *Journal of Materials Chemistry A*, 2014, **2**(19), P. 7082–7087.

[26] Byun D., Jin Y., Kim B., Kee Lee J., Park D. Photocatalytic TiO_2 Deposition by Chemical Vapor Deposition. *Journal of Hazardous Materials*, 2000, **73**(2), P. 199–206.

[27] Pradhan S.K., Reucroft P.J., Yang F., Dozier A. Growth of TiO_2 Nanorods by Metalorganic Chemical Vapor Deposition. *Journal of Crystal Growth*, 2003, **256**(1–2), P. 83–88.

[28] Baran E., YazIcI B. Effect of Different Nano-Structured Ag Doped TiO_2-NTs Fabricated by Electrodeposition on the Electrocatalytic Hydrogen Production. *International Journal of Hydrogen Energy*, 2016, **41**(4), P. 2498–2511.

[29] Cheng X., Pan G., Yu X. Visible Light Responsive Photoassisted Electrocatalytic System Based on CdS NCs Decorated TiO_2 Nano-Tube Photoanode and Activated Carbon Containing Cathode for Wastewater Treatment. *Electrochimica Acta*, 2015, **156**, P. 94–101.

[30] Ishikawa Y., Matsumoto Y. Electrodeposition of TiO_2 Photocatalyst into Nano-Pores of Hard Alumite. *Electrochimica Acta*, 2001, **46**(18), P. 2819–2824.

[31] Karuppuchamy S., Amalnerkar D.P., Yamaguchi K., Yoshida T., Sugiura T., Minoura H. Cathodic Electrodeposition of TiO_2 Thin Films for Dye-Sensitized Photoelectrochemical Applications. *Chemistry Letters*, 2002, **1**, P. 78–79.

[32] Ibrahim A., Mekprasart W., Pecharapa W. Anatase/Rutile TiO_2 Composite Prepared via Sonochemical Process and Their Photocatalytic Activity. *Materials Today: Proceedings*, 2017, **4**(5), P. 6159–6165.

[33] Arami H., Mazloumi M., Khalifehzadeh R., Sadrnezhaad S.K. Sonochemical Preparation of TiO_2 Nanoparticles. *Materials Letters*, 2007, **61**(23–24), P. 4559–4561.

[34] Guo W., Lin Z., Wang X., Song G. Sonochemical Synthesis of Nanocrystalline TiO_2 by Hydrolysis of Titanium Alkoxides. *Microelectronic Engineering*, 2003, **66**(1–4), P. 95–101.

[35] Yu J.C., Zhang L., Yu J. Direct Sonochemical Preparation and Characterization of Highly Active Mesoporous TiO_2 with a Bicrystalline Framework. *Chemistry of Materials*, 2002, **14**(11), P. 4647–4653.

[36] Selvam T.P., Kumar P.V., Saravanan G., Prakash C.R. Microwave-Assisted Synthesis, Characterization and Biological Activity of Novel Pyrazole Derivatives. *Journal of Saudi Chemical Society*, 2014, **18**(6), P. 1015–1021.

[37] Suwarnkar M.B., Dhabbe R.S., Kadam A.N., Garadkar K.M. Enhanced Photocatalytic Activity of Ag Doped TiO_2 Nanoparticles Synthesized by a Microwave Assisted Method. *Ceramics International*, 2014, **40**(4), P. 5489–5496.

[38] Magdalane C.M., Priyadharsini G.M.A., Kaviyarasu K., Jothi A.I., Simiyon G.G. Synthesis and Characterization of TiO_2 Doped Cobalt Ferrite Nanoparticles via Microwave Method: Investigation of Photocatalytic Performance of Congo Red Degradation Dye. *Surfaces and Interfaces*, 2021, **25**, P. 101296.

[39] Pol V.G., Langzam Y., Zaban A. Application of Microwave Superheating for the Synthesis of TiO_2 Rods. *Langmuir*, 2007, **23**(22), P. 11211–11216.

[40] Haider A.J., Jameel Z.N., Al-Hussaini I.H.M. Review on: Titanium Dioxide Applications. *Energy Procedia*, 2019, **157**, P. 17–29.

[41] Wang S., Zheng M., Jiang D., - al, Zhu Z., Wei K., Li H., Cai G., Chen Z., Qiang L. Synthesis and UV Detection Characteristics of TiO_2 Thin Film Prepared through Sol Gel Route. *IOP Conference Series: Materials Science and Engineering*, 2018, **360**(1), P. 012056.

[42] Rempel A.A., Kuznetsova Y.V., Dorosheva I.B., Valeeva A.A., Weinstein I.A., Kozlova E.A., Saraev A.A., Selishchev D.S. High Photocatalytic Activity Under Visible Light of Sandwich Structures Based on Anodic TiO_2/CdS Nanoparticles/Sol–Gel TiO_2. *Topics in Catalysis*, 2020, **63**(1–2), P. 130–138.

[43] Dorosheva I.B., Adiyak E.V., Valeeva A.A., Rempel A.A. Synthesis of Nonstoichiometric Titanium Dioxide in the Hydrogen Flow. *AIP Conference Proceedings*, 2019, **2174**, P. 020019.

[44] Kamalov R., Vokhmintsev A., Dorosheva I., Kravets N., Weinstein I. Synthesis of Composite Based on Carbon Nanotubes and Anodic Titania. *Advanced Science Letters*, 2016, **22**(3), P. 688–690.

[45] Rempel A.A., Kozlova E.A., Gorbunova T.I., Cherepanova S.V., Gerasimov E.Y., Kozhevnikova N.S., Valeeva A.A., Korovin E.Y., Kaichev V.V., Shchipunov Y.A. Synthesis and Solar Light Catalytic Properties of Titania-Cadmium Sulfide Hybrid Nanostructures. *Catalysis Communications*, 2015, **68**, P. 61–66.

[46] Wang Y., He Y., Lai Q., Fan M. Review of the Progress in Preparing Nano TiO_2: An Important Environmental Engineering Material. *Journal of Environmental Sciences (China)*, 2014, **26**(11), P. 2139–2177.

[47] El-Bahy Z.M., Ismail A.A., Mohamed R.M. Enhancement of Titania by Doping Rare Earth for Photodegradation of Organic Dye (Direct Blue). *Journal of Hazardous Materials*, 2009, **166**(1), P. 138–143.

[48] Humayun M., Raziq F., Khan A., Luo W. Modification Strategies of TiO_2 for Potential Applications in Photocatalysis: A Critical Review. *Green Chemistry Letters and Reviews*, 2018, **11**(2), P. 86–102.

[49] Gupta B., Melvin A.A., Matthews T., Dash S., Tyagi A.K. TiO_2 Modification by Gold (Au) for Photocatalytic Hydrogen (H2) Production. Renewable and Sustainable Energy Reviews, 2016, **58**, P. 1366–1375.

[50] Lenzmann F., Krueger J., Burnside S., Brooks K., Gra M., Gal D., Ru S., Cahen D. Surface Photovoltage Spectroscopy of Dye-Sensitized Solar Cells with TiO_2, Nb_2O_5, and $SrTiO_3$ Nanocrystalline Photoanodes: Indication for Electron Injection. *ACS Publications*, 2001, **105**(27), P. 6347–6352.

[51] Yanhong L., Dejun W., Qidong Z., Min Y., Qinglin Z. A Study of Quantum Confinement Properties of Photogenerated Charges in ZnO Nanoparticles by Surface Photovoltage Spectroscopy. *Journal of Physical Chemistry B*, 2004, **108**(10), P. 3202–3206.

[52] Kronik L., Shapira Y. Surface Photovoltage Phenomena: Theory, Experiment, and Applications. *Surface Science Reports*, 1999, **37**(1), P. 1–206.

[53] Xin B., Jing L., Ren Z., Wang B., Fu H. Effects of Simultaneously Doped and Deposited Ag on the Photocatalytic Activity and Surface States of TiO_2. *The Journal of Physical Chemistry B*, 2005, **109**(7), P. 2805–2809.

[54] Liqiang J., Dejun W., Baiqi W., Shudan L., Baifu X., Honggang F., Jiazhong S. Effects of Noble Metal Modification on Surface Oxygen Composition, Charge Separation and Photocatalytic Activity of ZnO Nanoparticles. *Molecular Catalysis*, 2006, **244**(1–2), P. 193–200.

[55] Chakrabarti S., Ganguli D., Chaudhuri S. Photoluminescence of ZnO Nanocrystallines Confined in Sol-Gel Silica Matrix. *Journal of Physics D: Applied Physics*, 2003, **36**(2), P. 146–151.

[56] Dorosheva I.B., Valeeva A.A., Rempel A.A. Sol-Gel Synthesis of Nanosized Titanium Dioxide at Various PH of the Initial Solution. *AIP Conference Proceedings*, 2017, **1886**(1), P. 020006.

[57] Dorosheva I.B., Weinstein I.A., Rempel A.A. Electrochemical and Sol-Gel Synthesis of Nanostructured Titania Photocatalyst Acting under Sunlight, 16TH IUPAC HIGH TEMPERATURE MATERIAL CHEMISTRY CONFERENCE (HTMC-XVI) Yekaterinburg, 2018, 272 p.

[58] Electroluminescent cell. Electroluminescent cell: patent 151492 Russia H05B 33/20 G01N 21/66. Vokhmintsev A.S., Fedorov M.D., Weinshtein I.A., patent holder. N 151492.59.

[59] Lu Y., Yuan M., Liu Y., Tu B., Xu C., Liu B., Zhao D., Kong J. Photoelectric Performance of Bacteria Photosynthetic Proteins Entrapped on Tailored Mesoporous WO_3-TiO_2 Films. *Langmuir*, 2005, **21**(9), P. 4071–4076.

[60] Liqiang J., Honggang F., Baiqi W., Dejun W., Baifu X., Shudan L., Jiazhong S. Effects of Sn Dopant on the Photoinduced Charge Property and Photocatalytic Activity of TiO_2 Nanoparticles. *Applied Catalysis B: Environmental*, 2006, 62(3–4), P. 282–291.

[61] Jing L., Li S., Song S., Xue L., Fu H. Investigation on the Electron Transfer between Anatase and Rutile in Nano-Sized TiO_2 by Means of Surface Photovoltage Technique and Its Effects on the Photocatalytic Activity. *Solar Energy Materials and Solar Cells*, 2008, **92**(9), P. 1030–1036.

Submitted 26 May 2023; revised 21 June 2023; accepted 22 June 2023

Information about the authors:

Irina B. Dorosheva – Ural Federal University, Mira str., 19, Yekaterinburg, 620002, Russia; Institute of Metallurgy of the Ural Branch of the Russian Academy of Sciences, Amundsena str., 101, Yekaterinburg, 620016, Russia; ORCID 0000-0001-9229-6758; i.b.dorosheva@urfu.ru

Alexander S. Vokhmintsev – Ural Federal University, Mira str., 19, Yekaterinburg, 620002, Russia; ORCID 0000-0003-2529-3770; a.s.vokhmintsev@urfu.ru

Ilya A. Weinstein – Ural Federal University, Mira str., 19, Yekaterinburg, 620002, Russia; Institute of Metallurgy of the Ural Branch of the Russian Academy of Sciences, Amundsena str., 101, Yekaterinburg, 620016, Russia; ORCID 0000-0002-5573-7128; i.a.weinstein@urfu.ru

Andrey A. Rempel – Ural Federal University, Mira str., 19, Yekaterinburg, 620002, Russia; Institute of Metallurgy of the Ural Branch of the Russian Academy of Sciences, Amundsena str., 101, Yekaterinburg, 620016, Russia; ORCID 0000-0002-0543-9982; rempel.imet@mail.ru

Conflict of interest: the authors declare no conflict of interest.